MODELICA Simulation-Based Probabilistic Assessment of i-SMR Containment Integrity under PCCS Performance Degradation

Seongjun Hong [a,b], Riyad Hasan [b], Yeon Ki Chung[b,c], Hyun Gook Kang[b*]
[a] *Dept. of Nuclear Engineering, Hanyang Univ., 222, Wangsimni-ro, Seongdong-gu, Seoul, 04763, Korea*
[b] *Dept. of Mechanical, Aerospace, and Nuclear Engineering, Rensselaer Polytechnic Institute, 110 8th St, Troy, NY 12180, USA*
[c] *Korea Institute of Nuclear Safety, 62, Gwahak-ro, Yuseong-gu, Daejeon, 34142, Korea*
[*] *Corresponding author: kangh6@rpi.edu*

Keywords: SMR, PCCS, LOCA, Dymola/Modelica, Sensitivity Analysis

1. Introduction

Small modular reactor (SMR) concepts emphasize passive safety to strengthen defense-in-depth and often adopt an integrated reactor configuration with a relatively small metallic containment vessel (CV). During a loss-of-coolant accident (LOCA), the passive containment cooling system (PCCS) is a key safety feature because it removes heat through condensation and boiling processes, thereby limiting containment pressurization. For example, in the Innovative SMR(i-SMR) designs, the reduced containment volume can lead to rapid pressurization in the early transient; therefore, containment integrity becomes closely coupled to PCCS performance.

In practice, however, passive system performance is subject to significant uncertainty. PCCS heat-transfer degradation may occur due to fouling of heat-exchanger surfaces, accumulation of non-condensable gases (NCGs), or other operational/aging mechanisms. Such degradation can increase the peak containment pressure demand, potentially eroding structural margins. Pre-determined deterministic safety analysis does not adequately reflect the continuous risk spectrum arising from partial performance degradation mechanisms. Therefore, a sensitivity analysis was conducted considering PCCS performance degradation and uncertainty in the pressure capacity of the containment vessel.

This study integrates Dymola simulations and probabilistic containment vessel structural pressure capacity modeling to quantify containment failure probability under two representative LOCA scenarios: a small-break LOCA (SB-LOCA) and a large-break LOCA (LB-LOCA). The accident conditions are established to cover the spectrum of break sizes required for design-basis accident (DBA) analysis, consistent with nuclear safety criteria [1]. The PCCS performance uncertainty is parameterized by a one-dimensional normalized performance variable and propagated through a surrogate model for peak pressure demand:

$$p = f_s(\mathrm{X}), s \in \{SB, LB\}, \mathrm{X} \in [0,1], \quad (1)$$

where p denotes the peak containment pressure demand, s indicates the scenario (SB or LB), and X represents normalized PCCS performance. Structural capacity is modeled as a lognormal random variable under saturated-steam conditions, with parameters adopted from a numerical investigation of i-SMR steel containment ultimate pressure capacity (UPC) result of Park et al. [2].

The failure data from repeated experiments with actual hardware is not available, thus the failure probability is evaluated via an expectation of the exceeding pressure capacity along the surrogate demand:

$$P_f(s) = \mathbb{E}[F_C(f_s(\mathrm{X}))], \quad (2)$$

Because the true distribution of PCCS performance is unknown, further a sensitivity screening is conducted by comparing three representative probabilistic assumptions corresponding to neutral, optimistic, and pessimistic performance scenarios. Furthermore, the one-dimensional formulation allows the failure probability to be evaluated directly via deterministic numerical integration, with its mathematical stability verified using the Cauchy convergence criterion.

2. Methods and Results

2.1 MODELICA simulation framework and accident scenarios

The system modeling was performed using the Modelica language in Dymola environment. The core thermal-hydraulic components were developed based on the TRANSFORM library [3] and the NHES library [4], which provide specialized models for nuclear hybrid energy systems. General components were adapted from the Modelica Standard Library and customized to meet i-SMR design specifications.

Two representative LOCA scenarios are considered: SB-LOCA and LB-LOCA for a safety injection line break. These scenarios are selected to envelop the limiting conditions for containment pressurization in accordance with standard safety analysis classifications [1]. For each scenario, a sweep of PCCS degradation levels is performed, and the peak containment pressure p is extracted as the primary load metric for structural reliability assessment.

2.2 PCCS performance uncertainty parameterization and surrogate demand model

2.2.1 Performance variable definition.

In this study, PCCS performance uncertainty is parameterized by a normalized effective cooling capability index. Physically, degradation mechanisms such as NCGs accumulation, surface fouling, or tube plugging result in a reduction of the overall heat transfer coefficient or effective surface area (UA). To model this macroscopic effect in Dymola, the number of active parallel tubes in the heat exchanger and conduction component was varied.

PCCS performance degradation is discretized into an effective performance index:

(3) $\mathrm{n} \in \{0,1,\dots,\mathrm{n_{max}}\},\ \mathrm{n_{max}} = 64,$

where $\mathrm{n} = 64$ represents nominal performance and $\mathrm{n} = 0$ represents a fully degraded PCCS. For probabilistic evaluation, a normalized continuous variable is employed:

(4) $\mathrm{X} \in [0,1],$

While the physical capacity is evaluated at discrete normalized states (n/n_{max}), X is introduced as a continuous surrogate parameter defined over the domain [0,1]. It represents the fraction of effective heat removal capacity remaining. This approach allows us to encompass various degradation scenarios into a single scalar metric for sensitivity analysis.

2.2.2 Surrogate for peak pressure demand.

Since the physical control parameter n is discrete, the solution space for PCCS performance is finite. In this study, exhaustive Dymola simulations are conducted for all feasible integer values of n from 0 to 64.

Consequently, the surrogate model $f_s(\mathrm{X})$ is constructed not as an approximation of a sparse dataset, but as a continuous representation of the complete solution space. A piecewise cubic Hermite interpolating polynomial (PCHIP) is employed to connect the 65 data points. This method guarantees that the surrogate curve passes exactly through every simulated data point, thereby introducing zero interpolation error at the physically realizable states.

The continuous form of $f_s(\mathrm{X})$ is utilized solely to facilitate probabilistic integration and to assess the sensitivity of the failure probability to continuous probability density functions of X.

The resulting surrogate models for SB-LOCA and LB-LOCA, alongside the discrete simulation data, are illustrated in figure 1. The plot demonstrates that the PCHIP approach captures the non-linear pressure response while accurately identifying the intersect point where SB-LOCA pressure begins to exceed LB-LOCA pressure.

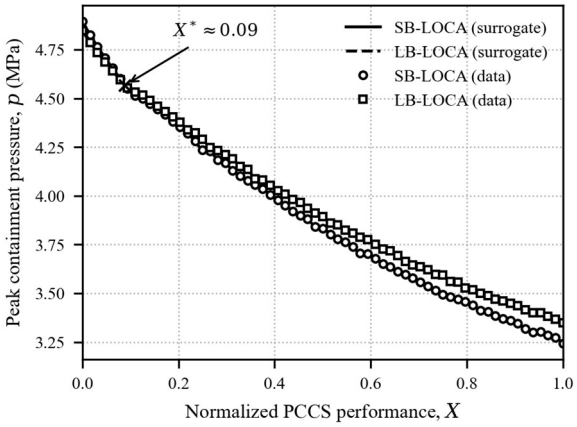

Fig. 1. Peak pressure vs PCCS performance surrogate. The PCHIP surrogate represents the discrete simulation data, capturing the SB-LB intersection point at X $\approx$ 0.09.

2.3 Structural capacity model under uncertainty

Containment pressure capacity C(UPC), defined as the threshold for structural rupture, is modeled as a lognormal random variable to reflect uncertainties in material properties and manufacturing tolerances. The fragility function is given by:

(5) $\mathrm{F_C(p)} = \mathbb{P}(\mathrm{C} < \mathrm{p}) = \Phi\left(\frac{\ln(\mathrm{p}/\mathrm{P_m})}{\beta_\mathrm{C}}\right),$

where Φ is the standard normal cumulative distribution function, $\mathrm{P_m}$ is the median capacity, and β_C is the logarithmic standard deviation.

The fragility parameters are determined to ensure both geometric accuracy and statistical consistency:

1. Median Capacity (P_m = 10.1324 MPa): Derived from high-fidelity finite element analysis results of Park et al. [2] performed on the identical i-SMR containment geometry.
2. Logarithmic Standard Deviation (β_C = 0.15): Estimated from equivalent steel structures [5]. While a baseline of 0.15 is selected to account for modeling uncertainties, sensitivity is further evaluated across a range of 0.12, 0.15, and 0.18.

2.4 Rare-event failure probability evaluation and screening

2.4.1 Expected-fragility formulation.

Containment failure is defined by the condition: $C < f_s(\mathrm{X})$. The scenario-conditional failure probability is therefore given by $P_f(s) = P(C < f_s(\mathrm{X}))$. Assuming C is statistically independent of X, this probability can be expressed as an expectation over PCCS performance uncertainty:

(6) $P_f(s) = \mathbb{E}_\mathrm{X}[P(C < f_s(\mathrm{X}) \mid \mathrm{X})] = \mathbb{E}_X[F_C(f_s(\mathrm{X}))].$

This formulation replaces binary failure indicators with averaging small probability values F_C (Eq.5) thereby substantially reducing estimator variance and improving numerical stability for rare-event probabilities on the order of $P_f \sim 10^{-8}$.

2.4.2 Distribution sensitivity screening for PCCS performance.

Because the true distribution of PCCS performance X is generally unknown, three representative screening assumptions are compared: Case U: X ~ Uniform(0,1), representing an evenly distributed performance. Case H: X~ Beta(5,2), representing an optimistic performance bias; Case L: X ~ Beta(2,5), representing a pessimistic performance bias; The distribution of these cases can be seen in figure 2.

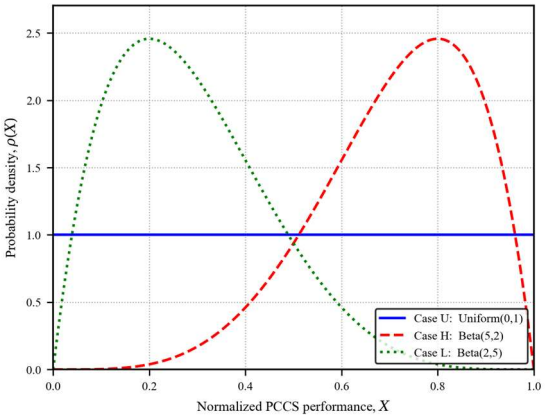

Fig. 2. Distribution of representative cases of PCCS performance distribution X.

2.5 Results

2.5.1 Peak pressure response and physical interpretation of SB-LB intersection.

As shown in Figure 1, an intersect is observed where the peak pressure of SB-LOCA exceeds that of LB-LOCA under severe PCCS performance degradation (X < 0.1), reaching a peak value of approximately 4.8 MPa. This response can be interpreted by considering both the phase condition of the break flow and the duration of mass release into the containment.

While LB-LOCA releases a larger total mass of coolant due to rapid blowdown, a significant portion of this effluent is in the liquid phase, which accumulates in the sump and contributes minimally to pressurization. In contrast, SB-LOCA exhibits slower depressurization, leading to two compounded effects: (1) it allows for phase separation within the primary side, resulting in a break flow with significantly higher steam quality, and (2) it substantially prolongs the duration of the coolant release before reaching the peak containment pressure.

When PCCS performance is nominal, this extended release of steam is effectively condensed over time. However, when PCCS heat removal is severely compromised (X $\rightarrow$0) the degraded condensation rate cannot compete with the ongoing steam generation. Consequently, the prolonged injection of high-quality steam in the SB-LOCA case yields a larger integrated vapor mass.

Parameter	LB-LOCA	SB-LOCA
Time to Peak Pressure	3,000 s	3,089 s
Total Discharged Mass	66,012 kg	51,571 kg
Liquid Mass in CV	44,017 kg	29,222 kg
Peak Vapor Mass in CV	21,994 kg	22,349 kg

Table A. Comparison of containment mass inventory and peak timing between LB-LOCA and SB-LOCA (Case of when X = 0)

This sustained vapor accumulation over longer period results in a higher steam partial pressure, ultimately causing the peak containment pressure to surpass that of the rapid, liquid-dominated LB-LOCA case

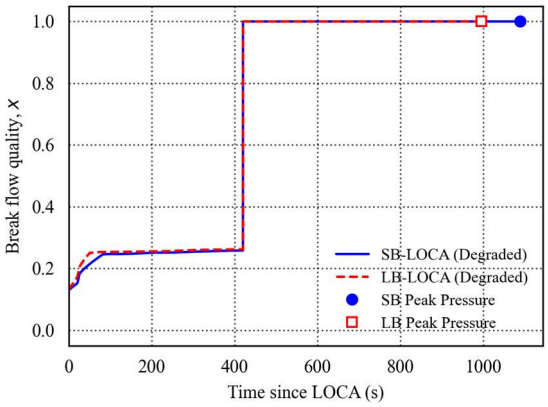

Fig. 3. LOCA flow quality for SB-LOCA and LB-LOCA. Markers denote the time of peak containment pressure (Case of when X = 0)

2.5.2 Capacity margin at the observed maximum load.

Figure 4 summarizes quadrature-based reference values of $P_f(s)$ (Eq. 6) under the three screening cases. In Case U, the failure probabilities are on the order of 10^{-8}. In case H, P_f decreases by 2–3 orders of magnitude from that of Case U, and SB-LOCA P_f is higher than LB-LOCA's (SB/LB<1). Conversely, Case L yields failure probabilities similar to those of Case U, with SB-LOCA maintaining a slightly higher risk than LB-LOCA.

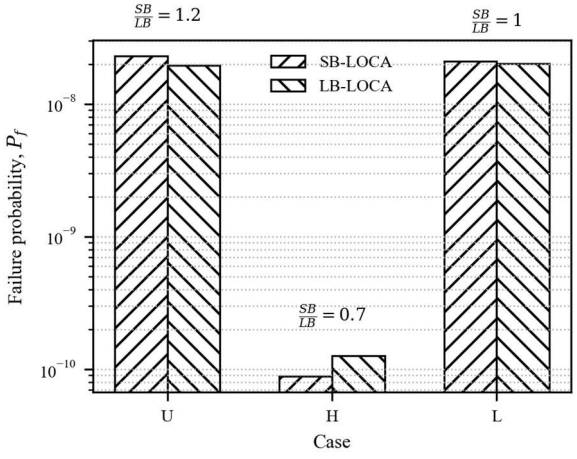

Fig. 4. P_f for Cases U/H/L on a log scale for SB and LB, with SB/LB ratio annotated.

The risk ranking can be explained by analyzing the cumulative risk contribution from the severely degraded region. As observed in Figure 1, the peak pressure of SB-LOCA exceeds that of LB-LOCA only when X < 0.1. Under Case U and Case L, this specific low-performance region (X < 0.1) dominates the overall risk profile, accounting for approximately 83–88% and 63–70% of the total P_f , respectively. Consequently, SB-LOCA exhibits a higher failure probability in these scenarios. Conversely, under the optimistic Case H assumption, the X < 0.1 region contributes less than 5% to the total P_f, shifting the dominant risk contributor to the higher X regions where LB-LOCA presents a greater pressure demand.

2.5.3 Sensitivity to structural capacity uncertainty.

Because P_f is sensitive to the tail of the capacity distribution, a sensitivity analysis was performed on the logarithmic standard deviation, β_C. As shown in Table B, varying β_C within a realistic range (0.12–0.18) results in a 5 to 7 order-of-magnitude shift in P_f. Although the relative risk ranking remains stable, the absolute magnitude shows that structural capacity is a source of uncertainty.

Distribution Case	LOCA Scenario	$\beta_C = 0.12$	$\beta_C = 0.15$ (Base)	$\beta_C = 0.18$
Case U (Uniform)	SB-LOCA	1.53×10^{-11}	2.31×10^{-8}	1.51×10^{-6}
	LB-LOCA	1.07×10^{-11}	1.96×10^{-8}	1.42×10^{-6}
Case H (Optimistic)	SB-LOCA	8.40×10^{-15}	8.89×10^{-11}	2.33×10^{-8}
	LB-LOCA	1.15×10^{-14}	1.27×10^{-10}	3.33×10^{-8}
Case L (Pessimistic)	SB-LOCA	9.32×10^{-12}	2.10×10^{-8}	1.77×10^{-6}
	LB-LOCA	7.56×10^{-12}	2.01×10^{-8}	1.81×10^{-6}

Table B. Sensitivity analysis results for varying β_C values across different distribution cases under LOCA.

3. Conclusions

This study assessed the structural reliability of an i-SMR containment under SB- LOCA and LB-LOCA by coupling MODELICA-based system simulations with a probabilistic capacity model. To efficiently estimate rare-event failure probabilities ($P_f \sim 10^{-8}$), a surrogate-based expected-fragility formulation was applied, $P_f(s)\ (Eq.2)$, which replaces binary failure counting with the continuous integration of small fragility values. Since in this study the PCCS performance uncertainty is assumed to be one-dimensional, this formulation was evaluated directly via deterministic numerical integration.

Under neutral screening assumption (Case U), failure probabilities are on the order of 10^{-8} for both small break LOCA and large break LOCA. The results are highly sensitive to the distribution assumption: Case H reduces P_f by approximately 2–3 orders relative to Case U. Importantly, the SB/LB risk ranking is assumption-dependent—SB-LOCA exhibits a higher failure probability than LB-LOCA under neutral and pessimistic assumptions, whereas the ranking reverses under the optimistic assumption.

These findings highlighted the importance of distribution screening and, ultimately, data-informed calibration when PCCS performance uncertainty is not well characterized. Although the current evaluation is based on existing design parameters, the framework is designed for adaptability. While the identified risk intersection was observed within the current simulation framework, its realization in a physical reactor environment warrants further empirical investigation. With future design updates, the P_f can be readily re-evaluated by regenerating the surrogate model $f_s(\mathrm{X})$ (Eq.1) with updated simulation data.

Future research will focus on calibrating PCCS performance distributions with empirical Integral Effect Test (IET) data and extend the framework to multi-dimensional uncertainty. Integrating scenario frequencies would enable a transition from conditional failure probabilities to the integrated risk metrics.

Acknowledgment

This work was supported by the Global Internship of the Korea Nuclear International Cooperation Foundation (KONICOF). The author is grateful to the Nuclear Plant Reliability and Information Laboratory (NPRI) at Rensselaer Polytechnic Institute (RPI) for their technical support and for providing the research environment.

REFERENCES

[1] U.S. Nuclear Regulatory Commission, "Standard Review Plan for the Review of Safety Analysis Reports for Nuclear Power Plants: LWR Edition," NUREG-0800, Section 6.2.1, "Containment Functional Design," Rev. 3, 2007.

[2] M. J. Park, H.S. Woo, D.H. Choi, and Y.S. Chang, “Numerical investigation on ultimate pressure capacity of a SMR containment vessel,” *Annals of Nuclear Energy*, vol. 220, art. no. 111530, Sep. 2025, doi: 10.1016/j.anucene.2025.111530.

[3] S. M. Greenwood, B. R. Betzler, and A. L. Qualls, "TRANSFORM: A Transient Simulation Framework of Reconfigurable Models," *Oak Ridge National Laboratory*, Oak Ridge, TN, USA, Rep. ORNL/TM-2017/163, 2017.

[4] S. M. Bragg-Sitton et al., "Nuclear-Renewable Hybrid Energy Systems: 2016 Technology Development Program Report," *Idaho National Laboratory*, Idaho Falls, ID, USA, Rep. INL/EXT-16-38161, 2016.

[5] L. Greimann, F. Fanous, and A. Saba, "Reliability Analysis of Containment Strength: Sequoyah and McGuire Ice Condenser Containments," *NUREG/CR-1891*, U.S. Nuclear Regulatory Commission, Washington, D.C., 1982.